Advanced Steel Construction – Vol. 17 No. 1 (2021) 1–9
DOI:10.18057/IJASC.2021.17.1.1

NUMERICAL STUDIES ON THE SEISMIC BEHAVIOUR OF A PREFABRICATED MULTI-STOREY MODULAR STEEL BUILDING WITH NEW-TYPE BOLTED JOINTS

Kashan Khan and Jia-Bao Yan *

School of Civil Engineering/Key Laboratory of Coast Civil Structure Safety of Ministry of Education, Tianjin University, Tianjin 300350, China
** (Corresponding author: E-mail: ceeyanj@163.com)*

ABSTRACT

Prefabricated modular steel (PFMS) construction is an industrial technique of construction that enhances productivity, site safety, and construction quality. The assembling of prefabricated buildings needs an accurate connecting system to ensure structural integrity and effective transfer of loads and moments. Therefore, in the current study, a new-type bolted joints having a long tenon-gusset plate for horizontally, and long beam bolts for vertically connecting modular units have been developed. Nonlinear static analysis was carried out by the finite element (FE) analysis software ABAQUS. The bending performance of the joints with varying parameters and modular units with different forces scenario, was studied. To analyse the seismic performance of modular steel building (MSB), a simplification of the detailed joint with the connector was performed. Then the seismic response of full-scale four-storey simplified MSB was studied by dynamic analysis. The results revealed that joints possessed stable load-carrying capacity with adequate ductility and seismic performance. The simultaneous application of axial, lateral tension, and compression forces affected ultimate capacity, initial stiffness, and ductility of single modules more than the double modules. Moreover, the simplified model accurately mimicked the bending behaviour of joints with a fluctuation of < 4% in capacities. Inter-storey drift ratios (IDR) of both the shorter and longer directions of MSB were found lower than the code limits of 2.5%. Hence, the static analysis on joints and modular units, and dynamic analysis on MSB authenticated the effectiveness of developed joints to resist and distribute the lateral loads. Finally, the accuracy of FE analysis was verified by analysing twelve bending tests on joints listed in the references.

ARTICLE HISTORY

Received: 7 April 2020
Revised: 23 September 2020
Accepted: 24 September 2020

KEYWORDS

New-type bolted joint;
Modular units;
Modular steel building;
Nonlinear static analysis;
Dynamic analysis;
Inter-storey drift ratio

1. Introduction

Prefabricated modular steel (PFMS) construction is an offsite construction in which structural members, panels, and facilities are preassembled in the factory to form modular units, then transported to the site and finally assembled to form the MSB [1,2]. Such construction technique, besides, the potential of dismantling and reusing, reduces assembling time, constructional wastage, maintenance cost, and also improves accuracy, material quality, and productivity in repetitive structures [3–5]. Nowadays, due to the economic sector and modern urbanization, prefabrication is gaining more attention in mid-to-high rise buildings compared to conventional onsite construction [3,6]. The construction technique, detailing requirements, and a various number of connections to assemble modular units to form MSB, make these buildings different from the traditional on-site steel buildings [7,8]. Based on the load transferring mechanism, modular units are mainly categorized into load-bearing, and corner-supported modules. Load-bearing modules use C-sectioned compression resisting walls to transfer gravity loads. In contrast, corner-supported modules use edge beams and columns to transfer both gravity and lateral loads [4,9]. The proper connection arrangement among modular units and appropriate lateral force resisting systems are essential for the transfer of lateral forces in MSB [10,11]. The primary purpose of connections in MSB is to provide alternate load-transfer paths and maintain structural integrity if severe damage to the adjacent structural components occurs [12,13]. The lateral bearing capacity of the joint consisted of supporting plate, and blind bolts was analysed by the cyclic loading, and finally, a simplified theoretical model based on the verified FE analysis was developed [14]. The seismic performances of exterior edge connection having a box with a threaded post-tensioned rod inserted in hollow structural section (HSS) columns were studied with a series of experiments [15]. Tensile and seismic behaviours of the proposed automatic plug-in connection in MSB were experimentally studied by Dai et al. (2019) [16]. The structural performance of the Vector Bloc joint was experimentally studied against axial and bending loads [1,17]. The rotational stiffness of the rotary joint in a modular structural system was investigated by experimental and theoretical ways by Chen et al. (2019) [18]. Lacey et al. (2019) experimentally studied the shear-slip and workability performance of the bolted joint, and FE analysis was carried out to explore the effect of various parameters [19]. The structural behaviour of the developed embedded column-foundation joint in MSB was analysed by experiments and FE analysis [10]. The influence of corrugated sidewalls (with and without openings) on the rigidity and seismic performance of MSB was analysed by experiments and detailed FE analysis [20,21]. The role of a new type of precast concrete core for being a new system to resist lateral forces was analysed under the wind and seismic loads by the use of FE analysis, and the response of the building was checked with the provided code provision [22,23]. The seismic performance of MSB frames, vertically connected by partial welding of columns and horizontally by angle clips and bolts, was evaluated using theoretical and experimental approaches [24,25]. Based on the experimental findings under monotonic lateral loading on the two-storey corner modular frame with and without the contribution of the corrugated shear wall, a theoretical derivation for the lateral stiffness of the modular system was proposed by Liu et al. (2020) [26]. The seismic response of a simplified MSB was analysed against pushover and dynamic analyses with the help of FE simulation [27]. The effect of a newly developed automatic interlocking system on the robustness performance of MSB was studied [3]. Zhang et al. (2020) investigated the bearing capacity of a full-scale modular unit under vertical and lateral loadings by using means of tests and FE analysis [28]. The studies previously recorded were found to be confined to the performance of corner joints, simplified frames or modular units without any proper detailed behaviour of connections, use of weaker sections and access holes, while, very least attention was paid to the behaviour of complex form of joints, i.e., middle joint, simplification of the joint to overcome computational efforts, combined effect of forces on the behaviour of modular units with the developed joint and the overall dynamic response of MSB against real earthquake accelerograms [8,24,25,27,29,30]. The main aim of the current study was to develop a new-type of bolted joint, analyse its bending performance, simplify and apply it in the full-scale modular units, and evaluate the overall seismic performance of the developed simplified multi-storey MSB.

Hence, in this study, a joint for HSS members was proposed. Using FE software ABAQUS, nonlinear structural behaviour of corner and middle joints was studied. In order to reduce the computational effort and evaluate the dynamic response of the MSB, a simplified model having a connector element as a replacement of joint, and the beam elements for solid structural members was developed. Then the structural performance of modular units against axial and lateral loads, while, MSB against earthquake loads were studied. This was followed by the validation of FE results with the results of twelve bending tests on joints in MSB. All the studies conducted led to a deeper understanding of the overall working process of the multi-storey MSB with such bolted joints.

2. Connecting and working mechanism of MSB with the developed joint

The details of connections in MSB are shown in Fig. 1(a), and the components of the developed joint are shown in Fig. 1(b). The joint mainly consists of the upper component, lower component, gusset plate (GP), beam, and column bolts for connecting modular units together. Beam bolts vertically, while, tenons, and GP horizontally connects the modular units together.

The force transfer mechanism showed by the joint against bending is shown in Fig. 2(b). The gap generation between the upper module and the lower module was notable when the bending moment was applied as a lateral displacement on the top of an upper modular frame. Due to gap generation,

beams, because of bending, started facing bearing stresses and beam bolts, due to stretching, faced tensile forces. Simultaneously, the relative movement among column, tenon, and column bolt resulted in the exertion of shear force on column bolts. It was observed that the overall structural behaviour of MSB depended on the working and load-transfer mechanism of the joint.

3. Experimental studies on the modular joints

The bending behaviour of corner and middle joints was studied against static and quasi-static loadings. The behaviour of joints was compared with and without stiffeners. The joint comprised hollow plug-in welded to plate, and long tension bolts passed through beams to horizontally and vertically support the welded HSS columns and beams [31,32].

3.1. Details of tests

The design of the connection was in accordance with the actual four-storey MSB built in China. Floor slabs of MSB were made of prefabricated concrete, while, lightweight composite boards were used to prepare partitions and ceilings. Both the ceiling boards and prefabricated floor slabs were connected to the inner face of beams using welded angles.

The main objective of the experiment was to analyse the structural behaviour, seismic performance, and load-carrying capacity of the proposed joint. Static loading, quasi-static loading, effect of diagonal stiffeners, cross-section of beams, and axial force ratio (AFR) were the main factors considered in the study. Twelve experiments were performed on six specimens of each corner and middle joints in the structural engineering laboratory of Tianjin University. Initially, four specimens for the joints, i.e., exterior and interior joints, were tested against monotonic loading to observe the lateral deformation and load-carrying capacity. Furthermore, eight specimens were tested against quasi-static loading to visualize the seismic performance of joints. The material properties and details of specimens are listed in Table 1 and 2. The specimens without stiffeners were used for the basic testing, whereas specimens reinforced with stiffeners used for parametric study. The lateral displacement of 100 mm using column-end technique was applied on the upper column with free end constrained condition, whereas floor beams (FB), ceiling beam (CB), and lower columns were pin-constrained. Chinese standard, “Regulation of seismic test method (JGJ101-96),” was used for quasi-static loading protocol. Two values of AFRs, i.e., 0.2 and 0.1, were considered for a comparative study.

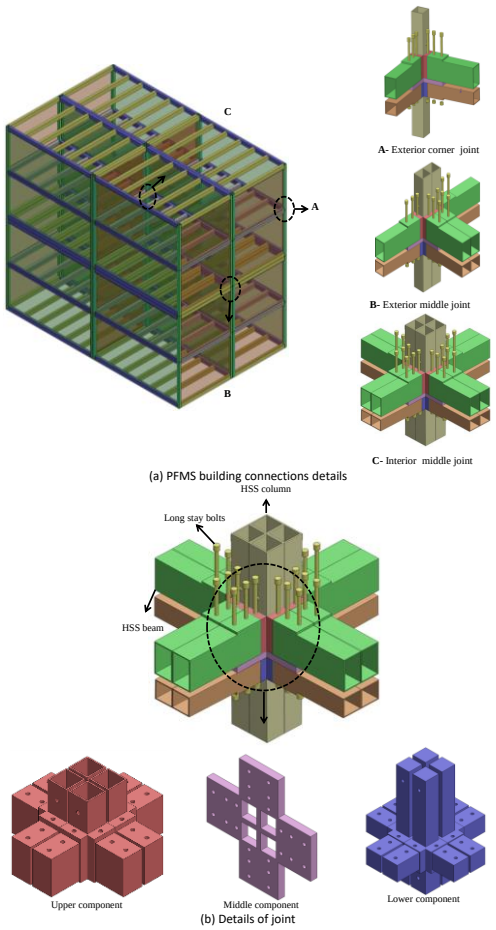

Fig. 1 Features of the developed connection in MSB

3.2. Material properties

The HSS columns, FBs, CBs, cover plates (CPs), supporting plates, GP, stiffeners, and beam bolts were made of Q345B steel, whereas cast steel Z35 was used for the production of connection components. Groove welding was adapted for the welding of columns and beams (FB, CB), while, fillet welding for stiffeners. The material properties listed in Table 1 were the same as the actual project.

4. Finite element model

4.1. General

Both ABAQUS/standard and dynamic-implicit types of solvers were considered for the development of FE models and analyses performed on the modular frame system with the developed joint. Lateral bending performance of new-type joints, simplified connector models, and modular units was studied using the tool of ABAQUS/standard. In contrast, the seismic performance of a simplified MSB with the developed connector model was analysed with a dynamic-implicit solver [33].

4.2. Material model of a steel

As steel was used in the study; therefore, the nonlinear isotropic/kinematic hardening model and von Mises yield criterion in ABAQUS/CAE were chosen. Bilinear stress-strain behaviour with strain hardening was used for defining the material model, as shown in Fig. 2(c) [34]. Poison’s ratio "ν" and modulus of elasticity "E_s" were defined as elastic material properties, whereas steel’s yield strength "f_y", strain values "ε" and ultimate strength "f_u" were inputted as plastic material properties. The elastic and plastic material properties used in the study were the same as experimental values, as shown in Table 1. The input criteria in FE simulation for the stress and strain are true stress and equivalent true plastic strain rather than engineering stress and strain. Therefore, values of true stress and strain can be obtained from the following equations using the values of engineering stress and strain.

$$\sigma_T = \sigma_E(1 + \varepsilon_E) \tag{1}$$

$$\varepsilon_T = \ln(1 + \varepsilon_E) - \frac{\sigma_T}{E_s} \tag{2}$$

where, σ_T and σ_E denote true and engineering stress, whereas ε_T and ε_E represent true and engineering strain.

Table 1
Properties of materials used in the experimental study

Components	Thickness (mm)	Yield strength f_y(MPa)	Ultimate strength f_u(MPa)	Elongation (% age)
Column & beam plate	8	425	575	30
Stiffeners	16	350	510	26
Cast plug-in device	-	330	350	22.5

4.3. Development of the FE model

In order to avoid modelling complications and reduce computational effort, some simplifications were considered in the FE models, such as a hexagonal head of bolts and nuts were modelled together as circular, while, threads on nuts and bolts shank were not modelled. The space between the bolt and the hole was not considered. In order to reduce contact surfaces and increase mesh accuracy, the welded CP and beams were modelled together as a single unit. The details of the FE model and simplifications adopted during simulations are shown in Fig. 2(a).

4.3.1. Meshing technique

The 3-D deformable solid parts, such as HSS columns, FBs, CBs, and connection components, were meshed with hexagonal- structured mesh controls having an element type of 8-node linear brick, controlled hourglass, and reduced integration (C3D8R). High-stress regions and components like corners, joining regions, bolt holes, and slave surfaces in contact definition were finely meshed. Four FE models with mesh densities, such as very fine, fine, coarse, and very

coarse with mesh sizes of 25, 30, 40, and 50 mm, were analysed against test conditions. The bearing capacity of the FE model was increased as the mesh size increased, i.e., from very fine mesh to coarse one, but the model with very coarse mesh showed a slight decrement in capacity compared to coarse one. The difference between capacities of coarse and very coarse mesh density models was not apparent. In contrast, the very fine mesh model stopped taking load farther than 73 mm and resulted in non-convergence, as shown in Fig. 5(a). Based on the detailed comparison between mesh convergence criteria and the test results, the accuracy of models with a fine mesh (mesh size of 30 mm) in both load-carrying capacity and stress allocation, authenticated the accuracy of FE models with the least error tolerance. Therefore, structural members were meshed with 30, a joint region with 10 and hole regions with the 8 mm. While, structural members such as columns and beams were substituted with 3-D deformable wire elements, which were finely meshed with the 2-node linear beam space element type (B31).

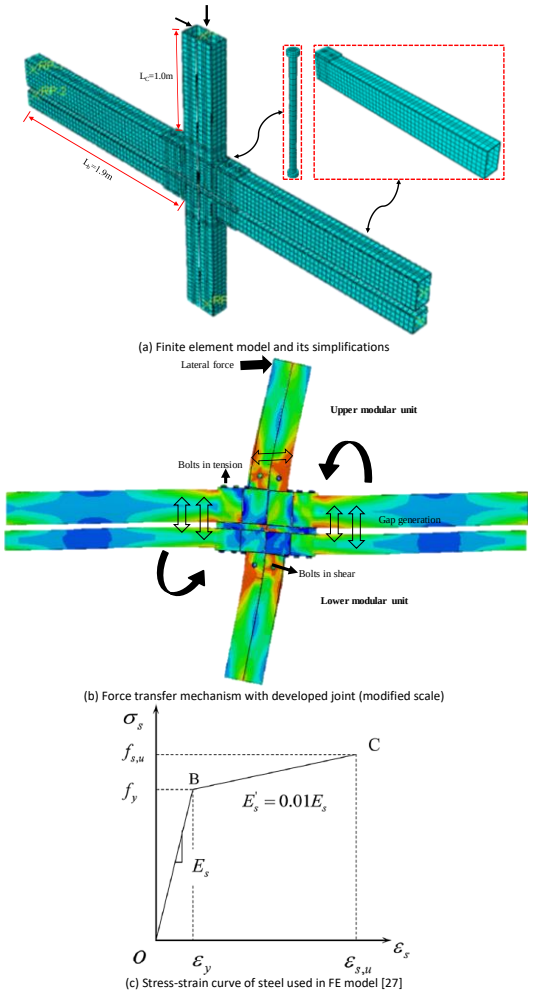

Fig. 2 Material properties and FE modelling details

4.3.2. Interactions

The interaction between column and connection, beam and connection, column and bolt, and beam and bolt were modelled as surface-to-surface (standard) with "hard contact" as normal behaviour and "finite sliding" by "penalty friction formulation" as a tangential behaviour. The hard-contact formulation causes the two interacting surfaces to exchange pressure when contact each other, while, no pressure transfer with surface separation. Whereas, penalty friction formulation considers the frictional coefficient that allows relative motion and determines the frictional force between contacting surfaces. The accurate friction coefficient was chosen after validating the results of FE analysis with experimental findings. For the purpose, two FE models (with and without bolts friction) were analysed, and there was a very slight increase of 0.006% in load carrying capacity was found in the FE model that considered bolts friction, as shown in Fig. 5(b). Similarly, FE models with four different friction coefficient values, such as 0.3, 0.4, 0.5, and 0.6, were analysed. An increase in the capacity of models was found as the friction coefficient increased, but the increase in capacity between models with a friction coefficient of 0.3 and 0.6 was about 1.5%, as shown in Fig. 5(c).

After the detailed comparison between FE and test results, bolts were modelled frictionless, whereas the friction coefficient was fixed as 0.3 for the remaining surface-to-surface interactions. For an accurate interaction between the adjacent modular units, the contact between columns and connections of adjacent modular units was considered as a hard contact.

4.3.3. Boundary conditions and load application situations

Following the bending experiments, movement at the bottom column in all directions, at the top column in X and Z direction, movement at FB and CB in Y, and the rotation in Z-direction was restricted. The displacement-controlled loading was applied in a downward direction to the top column, as shown in Fig. 2(a) and 2(b), respectively. The movement at the base of the modular units was restrained, while, the rotation was released in all three directions. Lateral tension, compression, and axial loads with two values of AFR, i.e., 0.1 and 0.2 calculated by Eq. (3), were used, as shown in Fig. 9. Factored dead load as a self-weight of the whole structure and the live load from ASCE 7-10 were applied on FBs of modular units and multi-storey MSB [13,35]. For dynamic analysis, the translation in all directions except the direction chose for studying the structural performance, was restrained, while, the rotation in all directions was released at the base of MSB. Ground motion accelerations of various earthquakes were applied at the base, as shown in Fig. 12(a). Following Eq. (4) was considered to calculate the pretension force for bolts.

$$N = (AFR) f_{yc} A_s \tag{3}$$

$$P = \frac{0.9 \times 0.9 \times 0.9}{1.2} A_e f_{tv} \tag{4}$$

where, N is Axial force; AFR is Axial force ratio in percentage; A_s is area of the steel section; P represents the pretension force; A_e denotes an effective area of the bolt, and f_{tv} shows the tensile strength of a bolt, which is taken as 180MPa.

Table 2
Information of the test specimens considered for the experiment

Sp. No	Type of joint	CB (mm^3)	FB (mm^3)	Column (mm^3)	Stiffener thickness (mm)	Bolts (mm)	AFR (%)	Loading method
S1	Exterior	150x150x8	150x250x8	150x150x8	None	24	0.2	Static
SC1	Interior	150x150x8	150x250x8	150x150x8	None	24	0.2	Static
S2	Exterior	150x150x8	150x250x8	150x150x8	10	24	0.2	Static
SC2	Interior	150x150x8	150x250x8	150x150x8	10	24	0.2	Static
QS1	Exterior	150x150x8	150x250x8	150x150x8	None	24	0.2	QS
QSC1	Interior	150x150x8	150x250x8	150x150x8	None	24	0.2	QS
QS2	Exterior	150x150x8	150x150x8	150x150x8	10	24	0.2	QS
QSC2	Interior	150x150x8	150x150x8	150x150x8	10	24	0.2	QS
QS3	Exterior	150x150x8	150x250x8	150x150x8	10	24	0.2	QS
QSC3	Interior	150x150x8	150x250x8	150x150x8	10	24	0.2	QS
QS4	Exterior	150x150x8	150x250x8	150x150x8	10	24	0.1	QS
QSC4	Interior	150x150x8	150x250x8	150x150x8	10	24	0.1	QS

4.4. Verification of the FE modelling

The load-displacement curves and failure patterns of twelve test specimens (i.e., S/SC/QS/QSC) of the corner and middle joints (with plug-in and long beam bolts) against monotonic (four specimens) and cyclic loadings (eight specimens) were compared with the results obtained from FE static analysis.

4.4.1. Verifications of experimental results with the FE analysis

The envelope load-displacement graphs for twelve test specimens of joints were compared with the results obtained from FE static analysis, as shown in Fig. 3. It was observed that the ultimate capacity, stiffness, and ductility of test specimens were well predicted by FE models. However, some minor fluctuations and inconstancies in stiffnesses or ultimate capacities between test and FE predicted curves were observed, which might be due to variation in material properties and behaviours, slight sectional imperfections during tests, dislocation during handling, flexible boundary conditions or simplifications performed during FE analysis.

The criteria of von Mises stress distribution were used to observe the failure modes of tests, as shown in Fig. 4. The main failure patterns observed in test specimens of joints, were gap generation and widening, tearing of welds of column or beam, stiffener breakage, local inward or outward buckling of the column, and tearing of column or beam. The stress concentrations showed by FE models in all specimens of joints (exterior and interior), local outward and inward buckling, welded regions under high stresses, and gap generation were following test results.

A comparison between the ultimate load-carrying capacities of tests and FE analysis, are shown in Table 3. The mean of capacity ratios of test and FE was found 1.02, while, SD and coefficient of variation (Cov) were 0.12, which assured the accuracy of FE analysis. Specimens with test-to-FE ratios higher than 1.0 demonstrated that FE analysis showed an average slight underestimation, whereas below 1.0 indicated that FE analysis showed an average slight overestimation of the bearing capacity. With these validations, the precision of the developed FE model can be authenticated to simulate the overall structural response of the joint, connected modular units, and MSB with a developed joint.

5. Numerical simulation of the modular frame systems

5.1. Geometry and detailing

In the Fig. (1b), the main components of the new-type of joint, such as an upper, lower, and middle component (GP), assembled with columns and beams to connect eight modular units with their respective components and bolts. The dimensions of the joint used to study the behaviour of MSB are shown in Fig. 6(a).

The structural performance of full-scale modular units, i.e., 6×3.6×2.9 m^3, was evaluated. After carrying out parametric studies considering the length of the respective column tenon, a length of 400 mm was initially chosen to investigate modular units, as shown in Fig. 9 [36]. Similarly, dimensions of full-scale four-storey simplified MSB with the detailed arrangement of connectors and details of boundary conditions are shown in Fig. 12(a).

5.2. Structural performance of joint

Nonlinear static analysis was conducted on FE models of the exterior corner and middle joints to evaluate the load-bearing capacity and the failure criteria of joints. Structural performance of joints (corner and middle), such as lateral bending capacities and stress accumulation, are shown in Fig. 7(a) and (b). It was observed that with a gradual increase of lateral displacement, load-carrying capacity linearly kept on increasing until the gap started generating between upper and lower modular beams, which resulted in beams yielding. Bearing stresses were developed in FBs with an increase in load. Finally, as the load reached the ultimate state, the system started dropping the capacity to take farther loading and remained stable for a while, which was then followed by bearing failure of FB. It was noted that both corner and interior joints showed stable ductile behaviour and prevented the failure of columns. In order to study the effect of two parameters, i.e., length of column tenon (such as 100, 200, 300, and 400 mm) and the constructional gap between adjacently connected modular units (such as from-0-to-30 mm) on the structural performance of joint, nonlinear static analysis was performed. It was noted that the length of tenon largely influenced the structural performance and load-carrying capacity, while, gap showed marginal influence, as shown in Fig. 7(c). Although, an increase in stiffnesses and load-carrying capacities of joints was evident with an increase in the length of tenon, the difference in increment decreased from 50 to 14% as the length of tenon increased between 100 to 200 and 300 to 400 mm. Moreover, the failure mode showed by the model with a length of tenon as 100 mm was controlled by column, while, in other models, FB faced bearing failure.

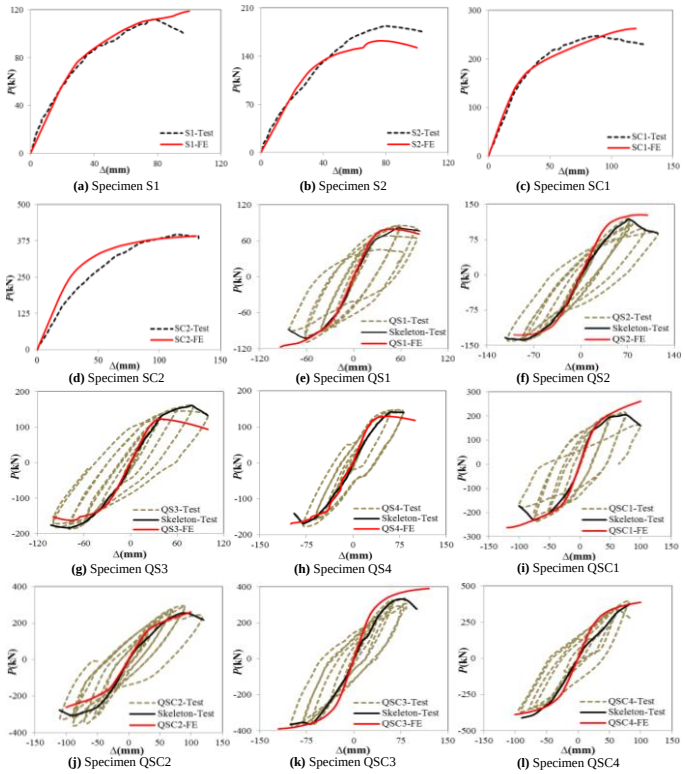

Fig. 3 Verification of load-displacement curves of test specimens with FE models

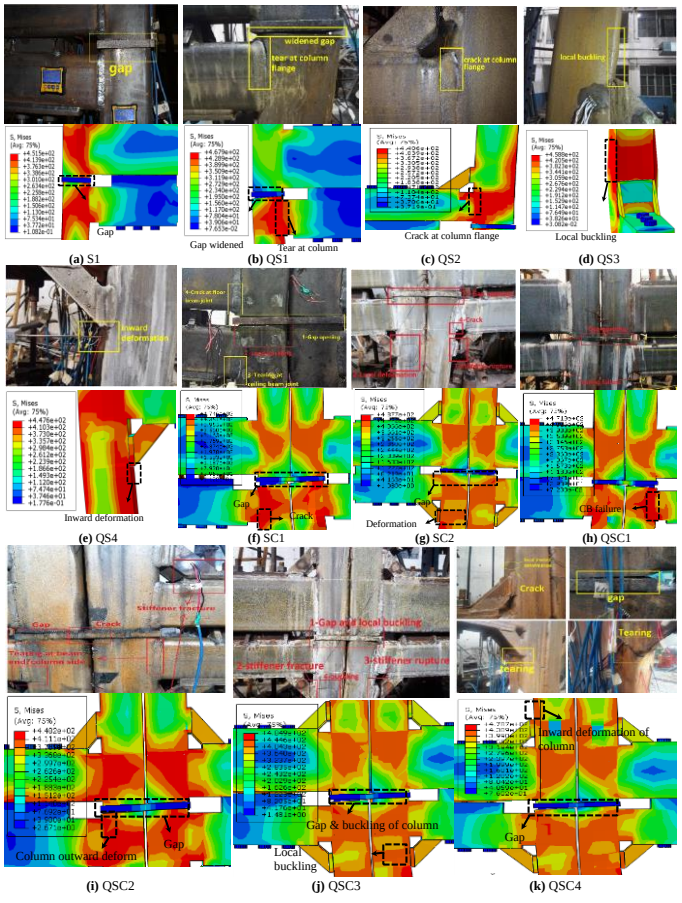

Fig. 4 Verifications of experimental results with the FE analysis

Table 3
Test-to-FE comparison of ultimate loadings

Sp. No	Type of joint	Loading technique	Ultimate load (Test)/P_{Test}(kN)	Ultimate load (FE)/P_{FE}(kN)	P_{Test}/P_{FE}
S1	Exterior	Static	112	118	0.95
SC1	Interior	Static	248	262	0.95
S2	Exterior	Static	183	162	1.13
SC2	Interior	Static	396	392	1.01
QS1	Exterior	QS +ve	81	79	1.02
		QS -ve	-102	-118	0.86
QSC1	Interior	QS +ve	205	261	0.79
		QS -ve	231	263	1.13
QS2	Exterior	QS +ve	118	121	0.97
		QS -ve	-137	-127	1.07
QSC2	Interior	QS +ve	255	261	0.98
		QS -ve	-305	-260	1.17
QS3	Exterior	QS +ve	161	122	1.32
		QS -ve	-183	-162	1.13
QSC3	Interior	QS +ve	329	391	0.84
		QS -ve	-364	-389	0.94
QS4	Exterior	QS +ve	141	129	1.09
		QS -ve	-168	-169	0.99
QSC4	Interior	QS +ve	377	387	0.97
		QS -ve	-411	-388	1.05
Mean					1.02
Cov					0.12

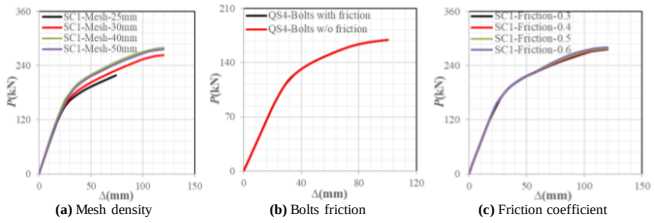

(a) Mesh density **(b)** Bolts friction **(c)** Friction coefficient

Fig. 5 Convergence study

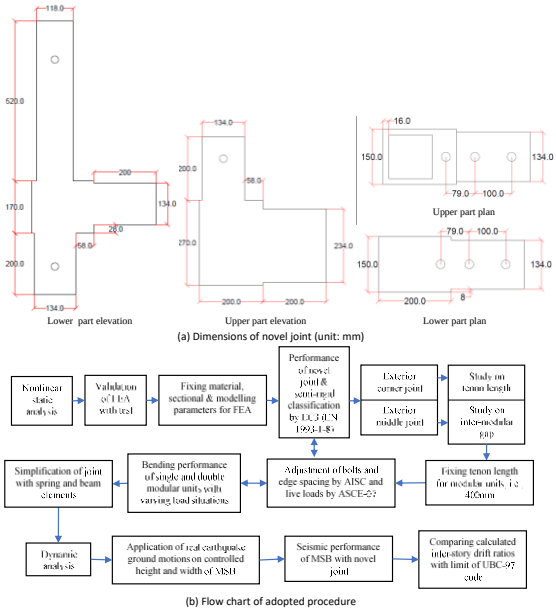

Fig. 6 Approaches adapted during FE analysis and design

5.3. Simplification of joint with the connector

For easy handling, reducing substantial computational effort, and analysing the structural performance of MSB, the complex and detailed FE model of the joint was simplified with the connector. In the simplified model, solid structural members, i.e., FBs, CBs, and columns, were replaced by 3-D beam elements, whereas components of joint with connector. The rotational stiffness for the connector was obtained from the moment-rotation relation of the detailed joint. Boundary conditions, material properties, sectional properties, and loading conditions were the same as for the analysis of the detailed FE model. The comparison of load-bearing capacities and stresses contours to analyse failure pattern of detailed solid and simplified beam element FE models of exterior corner joints are shown in Fig. 8(a), while, comparison for the exterior middle joint in Fig. 8(b). It was evident that the simplified models accurately predicted structural behaviour, stiffness, failure pattern, and load-carrying capacity of the detailed FE models of joints. The ratio of loading capacities of detailed and simplified FE models of joints with the error tolerance of less than 4% assured the accuracy of the developed simplified joint.

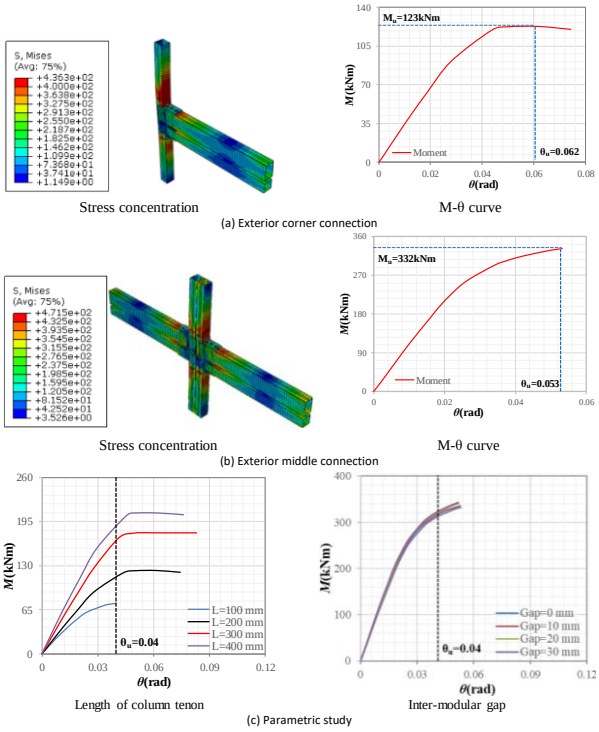

Fig. 7 Structural performance of developed joint

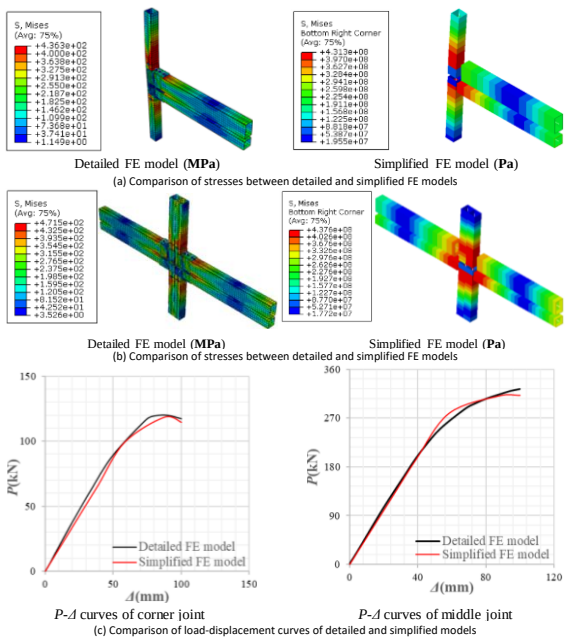

Fig. 8 Simplification of detailed joint

5.4. Structural performance of modular units with joint

The overall performance of full-scale single and double modular units was studied with varying force scenarios, as shown in Fig. 9. For a single modular unit, CBs were connected to the lower component, while, FBs with an upper component of joint without GP and intermediate tenons. Whereas, GP was used for horizontally connecting double modular units. Boundary conditions were applied to the centre of joints by adding reference points. Axial, lateral tension and compression or combination of axial, tension, compression forces were applied on single and double modular units. Axial force ratio of 0.1 was used for models SM-2 (single modular unit) and DM-2 (double modular unit), whereas 0.2 for models SM-3 and DM-3. The trial and error approach was adapted for obtaining the lateral elastic-plastic behaviour of modular units. The structural behaviours and load-carrying capacity of modular units are shown in Figs. 9 and 10. It was observed that models SM-3 and DM-3 (with AFR= 0.2, lateral tension and compression forces) showed the least load carrying capacity, whereas SM-6 and DM-6 (with only lateral compression force) showed the maximum bearing capacity. The ductility and load-carrying capacity possessed by double modular units were found better than the single modular units. Whether it was the single modular unit or double modular unit, the decrease in the number of loadings on modular units increased stiffness, bearing capacity, and ductility. The models observed bending of the column against tenons and beams against bolts, as shown in Fig. 2. The initial stiffnesses showed by models SM-1, SM-2, SM-3, SM-4, SM-5 and SM-6 were found increasing with order of 0.76, 0.76, 0.76, 1.05, 1.05 and 2.2 kN/mm, while, DM-1, DM-2, DM-3, DM-4, DM-5, DM-6 with 1.5, 1.5, 1.5, 2.0, 2.0 and 4.2 kN/mm. Bolts due to bending of beams faced shear stresses near heads, and beams faced bearing stresses against lateral displacement. Simultaneously, loss of stiffness was much obvious in single modular units, but double modular units showed force distribution among other structural members that highly increased the ductility performance. Similar structural behaviour was shown by SM-4 and SM-5, and DM-4 and DM-5. Nonlinearity in load-carrying behaviour was mainly due to a stress accumulation in CB and beam bolts.

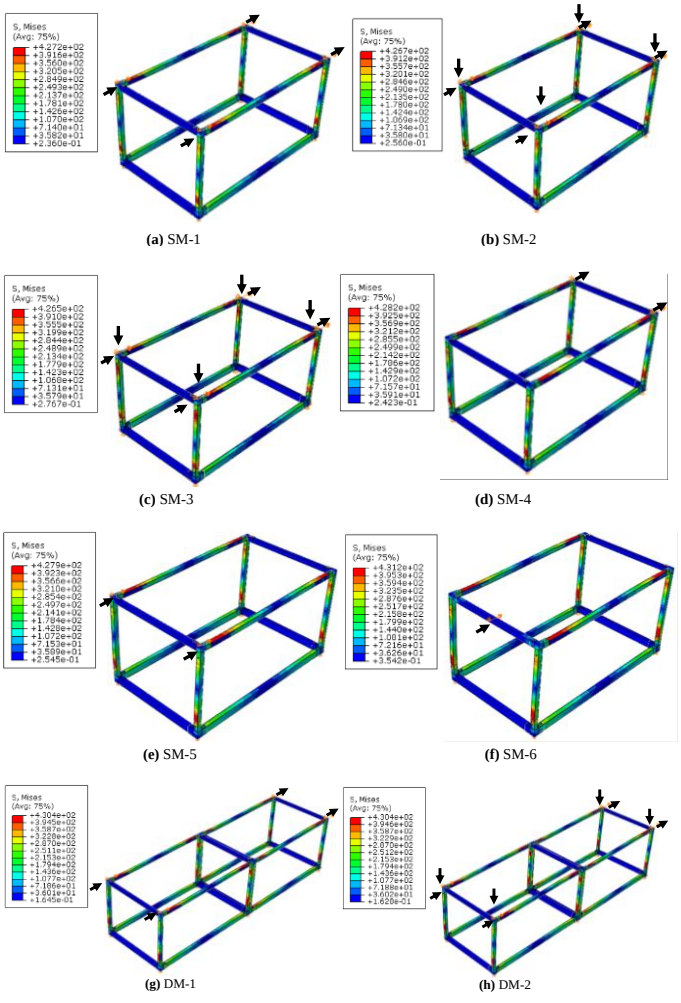

(a) SM-1 **(b)** SM-2 **(c)** SM-3 **(d)** SM-4 **(e)** SM-5 **(f)** SM-6 **(g)** DM-1 **(h)** DM-2

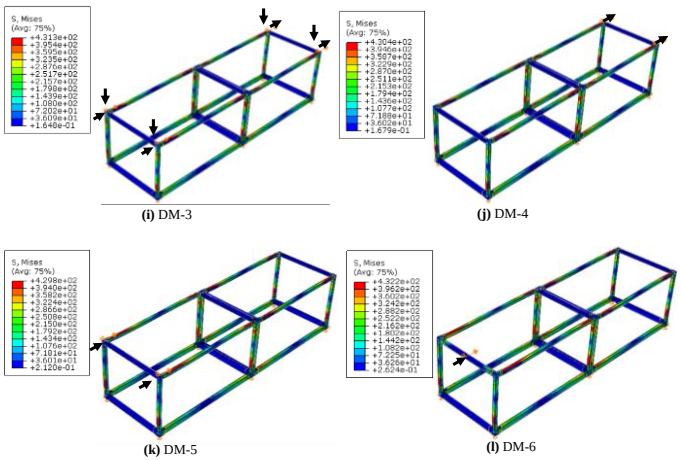

(i) DM-3 **(j)** DM-4 **(k)** DM-5 **(l)** DM-6

Fig. 9 von Mises stress distribution in single and double modular units

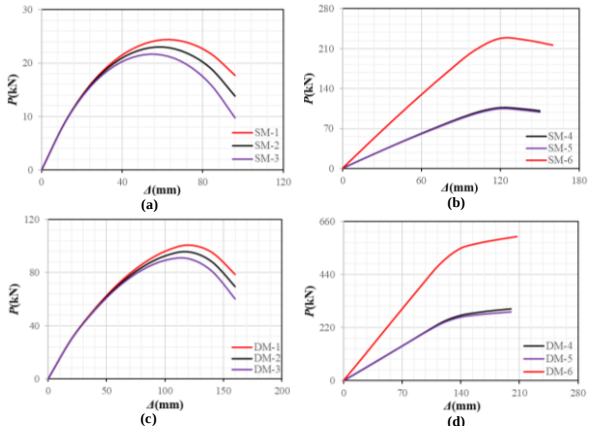

Fig. 10 Load-displacement curves of single and double modular units

5.5. Structural performance of a multi-storey MSB

In order to analyse the seismic performance of a developed MSB, a four-storey simplified building with twelve modular units was considered. As shown in Fig. 10, to study the seismic behaviour of MSB, ground motion accelerations of real earthquakes (scaled at 1/10th of real time) obtained from "PEER Strong Ground Motion Databases" were used for both along longer and shorter directions, as shown in Fig. 11 and 12(a). The details of applied ground motions in the current study are listed in Table 4. Edges of the columns (top and bottom) and adjacent modules were connected by coupling constraint. The rotation was released in all directions, whereas movement was fixed in all other directions except in the direction of the application of ground motions, as shown in Fig. 12(a).

For studying the seismic performance of MSB, two analyses were performed. Initially, eigenanalysis was carried out to find the natural frequency of various modes of the structure. Then dynamic implicit solver was used for studying the seismic behaviour of structure against accelerations of listed earthquakes. For damage in a structure, 5% damping ($\xi = 0.05$) was considered to find the damping coefficients, i.e., α= Mass proportion damping and β= Stiffness proportion damping. Using Eq.5, natural frequencies obtained from the linear perturbation analysis at lower modes, i.e., 1st and 3rd modes, were used to find α and β. The calculated damping parameters (α, β) were inputted in the material properties, and dynamic analysis was carried out using a dynamic-implicit solver. The same procedure was adapted for both longer and shorter directions. The inter-storey drift ratio, which is the normalization of the difference of lateral displacement of consecutive floors by the storey height, is the best response parameter for studying the damage of buildings [37]. The IDRs obtained with the response to various ground motions were compared with the allowable code limit (UBC-97) of 2.5% to examine the stability of MSB [38,39]. The IDRs obtained at each level and along both directions were represented in the Fig. 12(b). The pattern of IDRs along a shorter frame system was uniform with the longer frame system. In contrast, the average IDRs along a longer system were found averagely slightly larger than along a shorter system. The comparison of IDRs along both directions of frame systems was found lesser (0.3%) than the specified code limit of 2.5%, which ensured the safety of MSB with the

developed joint. The distribution of IDRs along the height and horizontal directions of the frames varied with each record in terms of amplitude and peak ground acceleration but they followed a very similar pattern.

$$\xi_x = \frac{\alpha}{2\omega_{ni}} + \frac{\omega_{ni}}{2}\beta \tag{5}$$

where, ξ_x= Damping (5%); α= Mass proportion damping; β= Stiffness proportion damping, and ω_{ni}= Natural frequency at i^{th} mode.

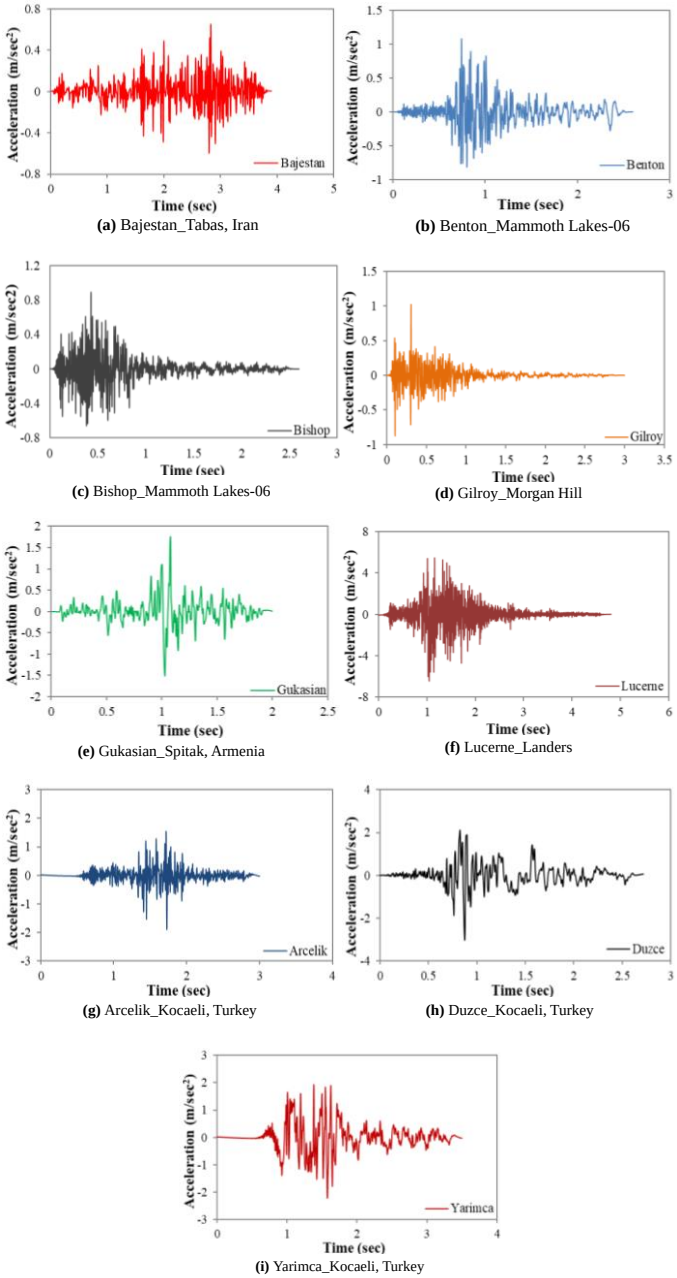

(a) Bajestan_Tabas, Iran **(b)** Benton_Mammoth Lakes-06

(c) Bishop_Mammoth Lakes-06 **(d)** Gilroy_Morgan Hill

(e) Gukasian_Spitak, Armenia **(f)** Lucerne_Landers

(g) Arcelik_Kocaeli, Turkey **(h)** Duzce_Kocaeli, Turkey

(i) Yarimca_Kocaeli, Turkey

Fig. 11 Scaled earthquake records considered in the study (1/10th)

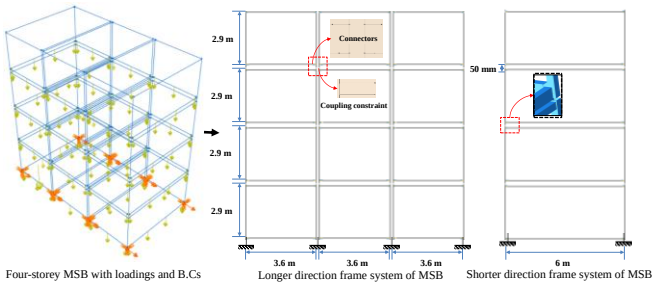

(a) Arrangement of spring connectors in PFMS frame system

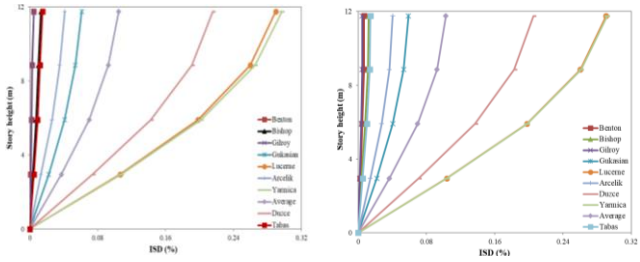

Along longer direction of MSB Along shorter direction of MSB

(b) Inter-storey drift ratios against various ground motions

Fig. 12 Structural performance of MSB with novel joint

Table 4
Record of considered ground motions

S.No	Station No	Earthquake name	Station name	Time (Year)	M_w	PGA (g)	Duration (sec)
1	56	Tabas, Iran	Bajestan	1978	7.35	0.029	39
2	430	Mammoth	Benton	1980	5.94	0.064	26
3	437	Mammoth	Bishop	1980	5.94	0.083	26
4	416	Morgan	Gilroy	1984	6.19	0.11	30
5	13	Spitak,	Gukasian	1988	6.77	0.12	20
6	25	Landers	Lucerne	1992	7.28	0.82	48
7	600	Kocaeli,	Arcelik	1999	7.51	0.08	30
8	709	Kocaeli,	Duzce	1999	7.51	0.21	27
9	1144	Kocaeli,	Yarimca	1999	7.51	0.24	35

6. Standard design and analysis approaches

For the detailed study on the structural performance of the modular frame system with developed joint, various standard analysis and design approaches were adopted. Material and sectional properties used in the FE analysis were chosen from experimental data [31,32]. The tenons in the joint were the main component for supporting columns and horizontally connecting modular units. The effect of tenon's length on overall structural performance and loading capacity was found evident. To evaluate the suitable length of tenon, the structural performance of the exterior corner connection with 1/10th, 1/5th, 1/3rd, and 1/2nd of column's length was studied. The study revealed that tenon showed an apparent increase in load-carrying capacity, but an increase in strength decreased from 50 to 14% as length increased from 100 to 400 mm. In accordance with the detailed analysis, the length of tenon was initially fixed for studying the performance of full-scale modular units. The purpose of nonlinear static analysis on joint and modular units was to obtain the forecasted lateral load-carrying capacity and failure pattern, and to provide relevant design recommendations. To obtain more realistic structural performance of modular units with the joint, performance of single and double modular units against various types of loadings was studied. The comprehensive study on structural performance suitably explained the behaviour, a structure may show with a developed joint. It was observed that beams and bolts controlled the failure behaviour; therefore, an appropriate design of edge distances and size or the number of bolts was needed.

To study the dynamic response and realistic seismic performance of MSB, ground motions of various catastrophic earthquakes were used in dynamic analysis. The simplified form of a joint (as discussed in section 5.3) with great accuracy made it easy to fully forecast the performance that a structure shows with such bolted joints in real earthquake situations. To study the stability effect, dynamic analysis was carried out on both horizontal directions of the frame system of MSB to find out important damage response parameters, i.e., IDR. The IDRs validated the safe behaviour showed by a low-storey MSB. The approaches adopted in analysis and design are shown in Fig. 6(b).

7. Discussions

Previously noted studies emphasized the importance of joints to resist lateral forces to ensure the integral and stable nature of MSB during catastrophic situations [12,13,20]. Therefore, in the current study, a new-type of the bolted joint was established, as shown in Fig. 1. The lateral bending performance of joints in terms of moment bearing capacity is presented in Fig. 7. The lateral load-carrying capacity showed by the joints was found comparatively better

than the joints proposed earlier [40,41]. According to the previous work done on the beam-column joints, joints with a plastic rotation angle greater than 0.032 rad were considered suitable and recommended in strong seismic zones [42]. Whereas, as per the seismic provisions provided by the American institute of steel construction (AISC), the minimum plastic rotation angle accumulation showed by the joints in special moment frames (SMF) must be greater than 0.04 rad [43]. It was observed that the developed joints (corner with 0.062 and middle with 0.053 rad) fulfilled the requirements of high seismic performance and can be applied as a lateral force-resisting system in MSB. The length of column tenons played a significant role in regulating the seismic performance joints (i.e., strong columns-weak beams and plastic rotation ≥ 0.04 rad), while, increasing the inter-modular gap possessed a nonapparent role, as shown in Fig. 7. The strength, i.e., $0.25M_P \leq M_j \leq M_P$ and stiffness classification criteria, i.e., $0.5EI_b/L_b \leq S_{ji} \leq 25EI_b/L_b$ for semi-rigid joints were listed in several studies [44–46]. The corner joint having single FB behaved as semi-rigid joint with strength > $0.5M_P$ (i.e. 88.8 kNm) and rotational stiffness > $0.5EI_b/L_b$ (i.e. 2749 kNm/rad), while, middle joint having two FBs showed strength > $0.5M_P$ (i.e. 177 kNm) and rotational stiffness > $0.5EI_b/L_b$ (i.e. 5498 kNm/rad). Therefore, the developed joint validated the previously reported research regarding semi-rigid conditions.

Previously, other researches showed the performance of individual and combined modular units with shear walls. They studied the effect of different loading scenarios and opening in walls on the stiffness of MSB. Still, less importance was paid to the contribution of joints in the overall performance of modular units, i.e., single and double with axial, lateral tension, and compression loads [47,48]. The information obtained from detailed bending performance showed that the joint in a single modular unit possessed the tendency to bear lateral loads with proper utilization of the strengths of members. The increase in capacities and stiffnesses of double modular units authenticated the fact that the load was bored and after the accumulation of plastic deformation, load and stresses were effectively transferred to the members of adjacent modular. Few kinds of research were reported on the seismic response of simplified low-storey MSB [6,8,27]. It was stated that MSB possessed better seismic response in terms of base shear and IDR (< 0.5% for 0.3g and < 1% for 2.0g in four-storey MSB) due to more number of structural members compared to the traditional steel buildings [15,27]. In the current study, the IDRs along both directions showed by four-storey low-rise MSB exhibited variation with each record based upon their amplitude and peak ground acceleration, but followed a very similar pattern, found in previous researches. The peak IDRs of < 0.3% showed by MSB in both directions against ground motions of highest (0.82g), median (0.24g), and lowest (0.029g) peak ground acceleration (PGA) were in good compliance with the reported work and code limits (< 2.5%).

8. Conclusions

This study aimed to analyse the structural behaviour of MSB with a new-type of the bolted joint. The frame system included the HSS column, FB, CB, GP, CP, and bolts made of Q345B steel, while, joint with ZG35. The function of GP in the corner modular system was to vertically separate the modular units, whereas, besides, vertical separation to keep modular units intact in the middle and interior frames horizontally. The nonlinear static analysis on the joint and modular units, while, dynamic analysis on full-scale MSB were performed. Discussions were made on the structural performance of joint, modular units, and full-scale four-storey MSB. The focus of the study was to observe the seismic behaviour of joint, modular units, and MSB using FE software, ABAQUS. The following conclusions were drawn from the FE analyses;

1) The validity of the FE models was accurately proved by comparing the bending results of twelve test specimens of joints with the results obtained from FE analysis.

2) Both corner and middle joints showed high bearing capacity, ductility, and satisfactory seismic performance, i.e., strong columns-weak beams and accumulation of plastic rotation angle greater than 0.04 rad. Although, length of column tenon showed fundamental effects on the capacities and failure behavior of models, effects showed by the inter-modular gap were nonapparent.

3) Simplified models of the connector and beam-elements accurately predicted the structural behaviour and moment-bearing capacities of detailed joints with the least error tolerance of < 4%. Simultaneously, the computational time and efforts were reduced to 90%.

4) Nonlinear static analysis on full-scale single and double modular units with different loading scenarios showed that double modular units possessed better ductile behaviour, bearing capacity, and initial stiffness compared to single modular units. The joint evidently showed a good tendency of the distribution of loads among connected structural components and prevented premature failure. In contrast, an increase in the number of loadings decreased the capacity of modular units.

5) Seismic response of four-storey MSB in both horizontal directions revealed that the values of average IDRs along the longer direction of the building were slightly more significant than the shorter direction. Still, both were under the code limit of 2.5%, which satisfied the safety requirements of low-rise MSB with the developed joint.

Acknowledgment

The authors are grateful for the scholarship provided by China scholarship council for the first author's study at Tianjin University.

List of notations

σ_T= True stress
σ_E= Engineering stress
ε_E= True strain
ε_T=Engineering strain
E_s= Modulus of elasticity of steel
N= Axial force
A_s= Area of section
f_{tv}= Tensile strength of the bolt
ω_i= Scale factor
φ_i= i^{th} mode
M_P= Plastic moment of the beam
P= Force of pretension in the bolt
A_e= Effective area of a bolt
P= Lateral load
Δ= Lateral displacement
θ= Angle of rotation
E_s= Elastic modulus of steel
μ= Frictional coefficient
P_{Test}= Ultimate load resisted by a test specimen
P_{FE}= Ultimate load resisted by the FE model
ξ_x= Damping (5%)
α= Mass proportion damping
β= Stiffness proportion damping
ω_{ni}= Natural frequency at i^{th} mode
S_{ji}= Rotational stiffness (kNm/rad)
M_j= Bending strength at the top of a column

Abbreviations

PFMS, Prefabricated modular steel; FE, Finite element; FB, Floor beam; Cov, Coefficient of variation; CB, Ceiling beam; HSS, Hollow structural section; CP, Cover plate; FS, Floor stringer; CS, Ceiling stringer; GP, Gusset plate; AFR, Axial force ratio; MSB, Modular steel building; IDR, Inter-storey drift ratio.

References

[1] J. Dhanapal, H. Ghaednia, S. Das, J. Velocci, Structural performance of state-of-the-art VectorBloc modular connector under axial loads, Eng. Struct. 183 (2019) 496–509. https://doi.org/10.1016/j.engstruct.2019.01.023.

[2] R. Jiang, C. Mao, L. Hou, C. Wu, J. Tan, A SWOT analysis for promoting off-site construction under the backdrop of China's new urbanisation, J. Clean. Prod. 173 (2018) 225–234. https://doi.org/10.1016/j.jclepro.2017.06.147.

[3] P. Sharafi, M. Mortazavi, B. Samali, H. Ronagh, Interlocking system for enhancing the integrity of multi-storey modular buildings, Autom. Constr. 85 (2018) 263–272. https://doi.org/10.1016/j.autcon.2017.10.023.

[4] R.M. Lawson, R.G. Ogden, R. Bergin, Application of modular construction in high-rise buildings, J. Archit. Eng. 18 (2012) 148–154. https://doi.org/10.1061/(ASCE)AE.1943-5568.0000057.

[5] M. Kamali, K. Hewage, Development of performance criteria for sustainability evaluation of modular versus conventional construction methods, J. Clean. Prod. 142 (2017) 3592–3606. https://doi.org/10.1016/j.jclepro.2016.10.108.

[6] R. Feng, L. Shen, Q. Yun, Seismic performance of multi-story modular box buildings, J. Constr. Steel Res. 168 (2020) 106002. https://doi.org/10.1016/j.jcsr.2020.106002.

[7] A.W. Lacey, W. Chen, H. Hao, K. Bi, Review of bolted inter-module connections in modular steel buildings, J. Build. Eng. 23 (2019) 207–219. https://doi.org/10.1016/j.jobe.2019.01.035.

[8] C.D. Annan, M.A. Youssef, M.H. El Naggar, Seismic vulnerability assessment of modular steel buildings, J. Earthq. Eng. 13 (2009) 1065–1088. https://doi.org/10.1080/13632460902933881.

[9] J.Y.R. Liew, Y.S. Chua, Z. Dai, Steel concrete composite systems for modular construction of high-rise buildings, Structures. (2019) 0–1. https://doi.org/10.1016/j.istruc.2019.02.010.

[10] K.S. Park, J. Moon, S.S. Lee, K.W. Bae, C.W. Roeder, Embedded steel column-to-foundation connection for a modular structural system, Eng. Struct. 110 (2016) 244–257. https://doi.org/10.1016/j.engstruct.2015.11.034.

[11] E.F. Deng, L. Zong, Y. Ding, Y.B. Luo, Seismic behavior and design of cruciform bolted module-to-module connection with various reinforcing details, Thin-Walled Struct. 133 (2018) 106–119. https://doi.org/10.1016/j.tws.2018.09.033.

[12] Y.S. Chua, J.Y.R. Liew, S.D. Pang, Robustness of Prefabricated Prefinished Volumetric Construction (PPVC) High-rise Building, (2018). https://doi.org/10.4995/asccs2018.2018.6955.

[13] P.M. Lawson, M.P. Byfield, S.O. Popo-Ola, P.J. Grubb, Robustness of light steel frames and modular construction, Proc. Inst. Civ. Eng. - Struct. Build. 161 (2008) 3–16. https://doi.org/10.1680/stbu.2008.161.1.3.
[14] B.H. Cho, J.S. Lee, H. Kim, D.J. Kim, Structural performance of a new blind-bolted frame modular beam-column connection under lateral loading, Appl. Sci. 9 (2019). https://doi.org/10.3390/app9091929.
[15] R. Sanches, O. Mercan, B. Roberts, Experimental investigations of vertical post-tensioned connection for modular steel structures, Eng. Struct. 175 (2018) 776–789. https://doi.org/10.1016/j.engstruct.2018.08.049.
[16] X.M. Dai, L. Zong, Y. Ding, Z.X. Li, Experimental study on seismic behavior of a novel plug-in self-lock joint for modular steel construction, Eng. Struct. 181 (2019) 143–164. https://doi.org/10.1016/j.engstruct.2018.11.075.
[17] J. Dhanapal, H. Ghaednia, S. Das, J. Velocci, Behavior of thin-walled beam-column modular connection subject to bending load, Thin-Walled Struct. (2019) 106536. https://doi.org/10.1016/j.tws.2019.106536.
[18] Z. Chen, Y. Liu, X. Zhong, J. Liu, Rotational stiffness of inter-module connection in mid-rise modular steel buildings, Eng. Struct. 196 (2019) 109273. https://doi.org/10.1016/j.engstruct.2019.06.009.
[19] A.W. Lacey, W. Chen, H. Hao, K. Bi, New interlocking inter-module connection for modular steel buildings: Experimental and numerical studies, Eng. Struct. 198 (2019) 109465. https://doi.org/10.1016/j.engstruct.2019.109465.
[20] Y. Ding, E.F. Deng, L. Zong, X.M. Dai, N. Lou, Y. Chen, Cyclic tests on corrugated steel plate shear walls with openings in modularized-constructions, J. Constr. Steel Res. 138 (2017) 675–691. https://doi.org/10.1016/j.jcsr.2017.08.019.
[21] Y. Yu, Z. Chen, Rigidity of corrugated plate sidewalls and its effect on the modular structural design, Eng. Struct. 175 (2018) 191–200. https://doi.org/10.1016/j.engstruct.2018.08.039.
[22] J. Bi, L. Zong, Q. Si, Y. Ding, N. Lou, Y. Huang, Field measurement and numerical analysis on wind-induced performance of modular structure with concrete cores, Eng. Struct. 220 (2020). https://doi.org/10.1016/j.engstruct.2020.110969.
[23] Z. Wang, W. Pan, Z. Zhang, High-rise modular buildings with innovative precast concrete shear walls as a lateral force resisting system, Structures. 26 (2020) 39–53. https://doi.org/10.1016/j.istruc.2020.04.006.
[24] C.D. Annan, M. Youssef, M.H. Naggar, Seismic performance of modular steel braced frames, 9h Can. Conf. Earthq. Eng. (2007). https://doi.org/10.13140/2.1.2132.2241.
[25] C.D. Annan, M.A. Youssef, M.H. El Naggar, Experimental evaluation of the seismic performance of modular steel-braced frames, Eng. Struct. 31 (2009) 1435–1446. https://doi.org/10.1016/j.engstruct.2009.02.024.
[26] Y. Liu, Z. Chen, J. Liu, Y. Bai, X. Zhong, X. Wang, Lateral stiffness evaluation on corner-supported thin walled modular steel structures, Thin-Walled Struct. 157 (2020) 106967. https://doi.org/10.1016/j.tws.2020.106967.
[27] A. Fathieh, O. Mercan, Seismic evaluation of modular steel buildings, Eng. Struct. 122 (2016) 83–92. https://doi.org/10.1016/j.engstruct.2016.04.054.
[28] J.F. Zhang, J.J. Zhao, D.Y. Yang, E.F. Deng, H. Wang, S.Y. Pang, L.M. Cai, S.C. Gao, Mechanical-property tests on assembled-type light steel modular house, J. Constr. Steel Res. 168 (2020) 105981. https://doi.org/10.1016/j.jcsr.2020.105981.
[29] S. Lee, J. Park, S. Shon, C. Kang, Seismic performance evaluation of the ceiling-bracket-type modular joint with various bracket parameters, J. Constr. Steel Res. 150 (2018) 298–325. https://doi.org/10.1016/j.jcsr.2018.08.008.
[30] S. Lee, J. Park, E. Kwak, S. Shon, C. Kang, H. Choi, Verification of the seismic performance of a rigidly connected modular system depending on the shape and size of the ceiling bracket, Materials (Basel). 10 (2017). https://doi.org/10.3390/ma10030263.
[31] Z. Chen, J. Liu, Y. Yu, C. Zhou, R. Yan, Experimental study of an innovative modular steel building connection, J. Constr. Steel Res. 139 (2017) 69–82. https://doi.org/10.1016/j.jcsr.2017.09.008.
[32] Z. Chen, J. Liu, Y. Yu, Experimental study on interior connections in modular steel buildings, Eng. Struct. 147 (2017) 625–638. https://doi.org/10.1016/j.engstruct.2017.06.002.
[33] ABAQUS (2013), User manual Version 6.13., DS SIMULIA Corp, Provid. RI, USA. (2013) 1–847.
[34] J.-B. Yan, Finite element analysis on steel–concrete–steel sandwich beams, Mater. Struct. 48 (2015) 1645–1667. https://doi.org/10.1617/s11527-014-0261-3.
[35] ASCE, ASCE STANDARD Loads for Buildings, 2010.
[36] R.M. Lawson, J. Richards, Modular design for high-rise buildings, Proc. Inst. Civ. Eng. - Struct. Build. 163 (2010) 151–164. https://doi.org/10.1680/stbu.2010.163.3.151.
[37] E. Miranda, S.D. Akkar, Generalized interstory drift spectrum, J. Struct. Eng. 132 (2006) 840–852. https://doi.org/10.1061/(ASCE)0733-9445(2006)132:6(840).
[38] S.R. Uma, A.B. King, T.J. Holden, D.K. Bell, Inter-storey Drift Limits for Buildings at Ultimate limit States, GNS Sci. Consult. Rep. 16 (2009) 1–33.
[39] Code, Uniform Building. “Uniform building code.,” 1997.
[40] S. Sup, K. Woong, K. Sung, S. Yub, An Experimental Evaluation of Structural Performance for the Beam to Column Joints in Unit Modular System, J. Korean Soc. Steel Constr. 25 (2013) 255–265. https://doi.org/10.7781/kjoss.2013.25.3.255.
[41] Lee, Behavior of C-Shaped Beam to Square Hollow Section Column Connection in Modular Frame, J. Korean Soc. Steel Constr. 27 (2015) 471. https://doi.org/10.7781/kjoss.2015.27.5.471.
[42] X.C. Liu, A.X. Xu, A.L. Zhang, Z. Ni, H.X. Wang, L. Wu, Static and seismic experiment for welded joints in modularized prefabricated steel structure, J. Constr. Steel Res. 112 (2015) 183–195. https://doi.org/10.1016/j.jcsr.2015.05.003.
[43] B. Taranath, Seismic Provisions for Structural Steel Buildings, ANSI/AISC 341-10, Struct. Anal. Des. Tall Build. (2011) 355–410. https://doi.org/10.1201/b11248-8.
[44] EN 1993-1-1, Eurocode 3: Design of steel structures - Part 1-1: General rules and rules for buildings, 2005. https://doi.org/[Authority: The European Union Per Regulation 305/2011, Directive 98/34/EC, Directive 2004/18/EC].
[45] Y. Wang, J. Xia, R. Ma, B. Xu, T. Wang, Experimental Study on the Flexural Behavior of an Innovative Modular Steel Building Connection with Installed Bolts in the Columns, Appl. Sci. 9 (2019) 3468. https://doi.org/10.3390/app9173468.
[46] K.-S. Choi, H.-J. Kim, Analytical Models of Beam-Column joints in a Unit Modular Frame, J. Comput. Struct. Eng. Inst. Korea. 27 (2014) 663–672. https://doi.org/10.7734/coseik.2014.27.6.663.
[47] Y. Zuo, X. Zha, FEM and experimental study on mechanical property of container building with holes, Int. J. Steel Struct. 17 (2017) 175–194. https://doi.org/10.1007/s13296-015-0132-y.
[48] K. Giriunas, H. Sezen, R.B. Dupaix, Evaluation, modeling, and analysis of shipping container building structures, Eng. Struct. 43 (2012) 48–57. https://doi.org/10.1016/j.engstruct.2012.05.001.